

# Blind Image Deblurring via Regularization and Split Bregman

Su Xiao, Fangzhen Ge, and Ying Zhou

**Abstract**—Degradation caused by blurring is ubiquitous in digital images, and blind image deblurring (BID) has been proposed to solve this issue. Over the past several decades, various techniques and tools have been developed for BID problems, and continual efforts have been made to improve the speed and accuracy of sharp image estimation. This study proposes a new BID method, which incorporates a regularization technique, sparsity-inducing priors, and the split Bregman method. In the first phase, the proposed method equates blur estimation with a constrained minimization problem in which sparsity-inducing priors are employed to regularize the gradient image and blur the kernel. The split Bregman method is then applied to divide and conquer the minimization problem to optimize the blur estimation. To enhance the accuracy of the outputs, a coarse-to-fine updating procedure is integrated into the Bregman iterations. The resulting subproblems are efficiently addressed during the alternating iteration by employing methods such as the fast Fourier transform (FFT) and hard shrinkage. In the second phase, the total variation (TV) deconvolution model is applied to sharp image reconstruction, and a classic half-quadratic approach is applied to handle the model with high efficiency. In our experiments, the proposed method and three similar methods are employed to deal with synthetic blurry images and real-world blurry images from open image databases. The deblurring results are presented in the form of recovered images and peak signal-to-noise ratio (PSNR) values. To compare speed performances, the computation times for image deblurring are computed and reported. The proposed method can be applied to efficiently handle various types of blurry images and produce satisfactory outputs. Experimental outputs indicated that the proposed method provides superior restoration quality and computing speed compared with alternatives.

**Index Terms**—blind deblurring, regularization technology, sparse inducing, split Bregman, hard shrinkage.

## I. INTRODUCTION

**B**LUR has always been a problem for digital images and is becoming increasingly serious with the popularization of handheld imaging devices. Hence, research on blind image deblurring (BID) has received increased attention. In the field of BID, a blurry image is expressed as  $Y = B \otimes X + N$  where  $Y$  is the blurry image;  $B$  and  $X$  are the unknown blur kernel and sharp image, respectively;  $\otimes$  is the convolution operator; and  $N$  is the noise. In recent years, researchers have successfully presented many effective BID methods. Most of these methods can be classified as

variational Bayesian (VB) methods [1-4], TV-regularized methods [5-8], and sparse representation (SR) based methods [10-13].

Likas et al. [1] were the first to apply a Bayesian framework to solve the BID problem. To find closed-form solutions for the Bayesian BID model, the authors adopt a variational approximation approach derived from expectation maximization. Fergus et al. [2] use a similar methodology to that of [1], but with differences in prior knowledge and estimation strategy. To avoid the shortcomings of the blur estimation method used in [1] and [2], Tzikas et al. [3] propose modeling the point spread function by using a sparse-kernel prior, which allows for estimating the support of the blur kernel and encourages smooth blur. Zhou et al. [4] divide the BID problem into two phases, i.e., image restoration and blur estimation, and utilizing alternating minimization and the variational Dirichlet process, respectively, to deal with them. With the help of the nondimensional Gaussian measure and the Dirichlet distribution, this method yields good performance in terms of alleviating artifacts and removing kernel noise. In general, the performances of the VB methods rely significantly on the selection of prior distribution models and variational approximation approaches.

An attractive tool, TV has been successfully used in many image processing fields. To achieve image edge recovery and efficient blur estimation, Chan et al. [5] introduce TV into the BID problem but fail to properly tackle the numerical computing problems of the TV-regularized model. Li et al. [6] employ split Bregman iteration to improve the TV-regularized BID model presented by Chan et al. in [5]. To regularize the blur kernel, Liu et al. [7] construct a new convex regularizer, in which the TV-based prior is still imposed on a sharp image, to replace the TV-regularizer in the BID model of Chan et al. Similarly, to refine the classic TV-regularized model presented in [5], Liu et al. [8] substitute a new data-fidelity term for the original and handle the new TV-regularized model with a weighted approach that aims to perform image deblurring rapidly. For TV-regularized methods, in addition to the challenges posed by the numerical computation of the TV-regularizer, the deblurred results are influenced by initial settings [9].

The so-called transform sparsity of images is the rationale behind the SR technology that creates many of the representative BID methods. Transform sparsity means that an image can be represented by the least number of coefficients in a transform domain such as the Fourier domain or the wavelet domain. Cai et al. [10] utilize a framelet system to code the sharp images and blur kernel. The  $l_1$ -norms of the resulting coefficients serve as the regularized terms. Because of its sparseness, the blur kernel rarely includes helpful information for estimation in coding. Based on a fusion of the low-rank, nonlocal similarity, and sparse priors, Ren et al.

Manuscript received February 10, 2018; revised September 2, 2018. This work was supported by Anhui Provincial Natural Science Foundation (Grant No. 1608085QF150) and Natural Science Research Project of the Education Department of Anhui Province (Grant No. KJ2018A0397).

Su Xiao is with the School of Computer Science and Technology, Huaibei Normal University, Huaibei 235000, China (e-mail: csxiaosu@163.com).

Fangzhen Ge is with the School of Computer Science and Technology, Huaibei Normal University, Huaibei 235000, China (e-mail: gzfz203377@163.com).

Ying Zhou is with the School of Computer Science and Technology, Huaibei Normal University, Huaibei 235000, China (e-mail: yingzhou@sohu.com).

[11] construct a new BID model whose cost function includes as regularizers the quadratic  $l_2$ -norm of the blur kernel and  $l_0$ -norm of the gradient image. Like Ren et al., Yu et al. [12] resort to an alternating optimization strategy to estimate unknowns in their BID problem. Comparatively speaking, because BID is cast as a smooth minimization problem, the BID work in [12] may be easier to complete. With a focus on disposing of text images, Pan et al. [13] model the BID problem as a novel optimization problem that enforces  $l_0$ -norm-based priors on the sharp image and its gradient. The researchers present an edge-based method for addressing this optimization problem.

Although new theories and methods are being proposed, the efficient and accurate estimation of sharp images and blur kernels still encounter obstacles due to the inherently ill-posed nature of BID problems. An efficient BID method is proposed in this study to estimate the sharp image and blur kernel. The proposed method solves the BID issue in two phases. The first phase jointly estimates the gradient image and the blur kernel in an alternating process, and the second phase performs deconvolution to obtain the sharp image based on the blur estimation output. The remainder of the paper is structured as follows: In Section 2, the proposed two-phase BID is described in detail. Section 3 is the experimental section, wherein a comparative analysis is carried out among several BID methods. The last section draws conclusions.

## II. PROPOSED BID METHOD

Regarding the ill-posed problems described above, Tikhonov et al. [14] suggest using regularization as the solver, and the last few decades have witnessed many successful applications of regularization to the solution of inverse problems in imaging. In the context of regularization, BID problems can be uniformly written as

$$\min_{B,X} \{J(B, X) = Q(B, X) + \Phi_1(B) + \Phi_2(X)\}, \quad (1)$$

where  $J(B, X)$  is the cost function; the first term of  $J(B, X)$  is a data-fidelity term that maintains the consistency of the sharp and blurry image; and  $\Phi_1(B)$  and  $\Phi_2(X)$ , called regularizers or regularized terms, are used to guarantee that the BID problem converges in a stable manner to a nontrivial solution. Early methods (e.g., [15]) tend to adopt  $\|B\|_2^2$  and  $\|LX\|_2^2$  as regularizers, recovering overly smoothed sharp images. Subsequent TV-regularized and sparsity-inducing models can effectively avoid this issue, and they have become the mainstream options for solving BID problems.

As illustrated by Eq. (1), BID methods aim to restore sharp images and blur kernels from given blurry images. This study suggests a two-phase processing strategy to achieve this goal.

### A. Blur Estimation

Given that the prominent edges of intermediate images contribute to precisely estimating the blur kernel, the proposed method formulates blur estimation as

$$\min_{U,B} \frac{1}{2} \|B \otimes U - W\|_2^2 + \mu_1 \|B\|_0 + \mu_2 \|U\|_0, \quad (2)$$

s.t.  $b_i \geq 0, \sum_i b_i = 1$

where  $U = (\nabla_h X, \nabla_v X)^T$  and  $W = (\nabla_h Y, \nabla_v Y)^T$  are the gradients of the sharp image  $X$  and blurry image  $Y$ , respectively;  $\nabla_h$  and  $\nabla_v$  are the gradient operators in the horizontal and vertical directions, respectively;  $\|\cdot\|_0$  denotes the sparsity-inducing  $l_0$ -norm, as it calculates the number of nonzero elements, whereas  $l_0$ -norm is fairly appropriate for measuring the natural sparsity of the gradient image and blur kernel; and the penalty weights  $\mu_1$  and  $\mu_2$  are positive constants and regulate the strength of regularization. With  $b_i$  denoting an arbitrary element of  $B$ ,  $b_i \geq 0$  and  $\sum_i b_i = 1$  are the nonnegative and normalized constraints, respectively, which stem from the natural attributes of the blur kernels.

Directly handling the minimization problem (2) is illogical given the  $l_0$ -norm and two known variables in its cost function. To settle minimization problems such as problem (2), many BID methods resort to simply alternating minimization schemes to approximate the optimum solutions. However, compared with the newly emerging split Bregman approach [16-17], alternating minimization tends to be gradual, unstable, and insufficiently accurate. Therefore, this paper adopts the split Bregman method to dispose of problem (2) and estimate the blur kernel in a low-overhead and high-speed manner. The split Bregman method combines variable splitting and Bregman iteration [18] and has demonstrated unique advantages in image processing [19-21]. Through variable splitting, the split Bregman method first converts problem (2) into the following equivalent problem:

$$\min_{U,B,S,Z} \frac{1}{2} \|B \otimes U - W\|_2^2 + \mu_1 \|Z\|_0 + \mu_2 \|S\|_0. \quad (3)$$

s.t.  $b_i \geq 0, \sum_i b_i = 1, Z = B, S = U$

Afterwards, Bregman iteration decouples problem (3) into a series of subproblems:

$$B^{k+1} = \underset{B}{\operatorname{argmin}} \|B \otimes U^k - W\|_2^2 + \lambda_1 \|B - Z^k - D_1^k\|_2^2, \quad (4)$$

s.t.  $b_i^{k+1} \geq 0, \sum_i b_i^{k+1} = 1$

$$Z^{k+1} = \underset{Z}{\operatorname{argmin}} \frac{\lambda_1}{2} \|B^{k+1} - Z - D_1^k\|_2^2 + \mu_1 \|Z\|_0, \quad (5)$$

$$D_1^{k+1} = D_1^k + B^{k+1} - Z^{k+1}, \quad (6)$$

$$U^{k+1} = \underset{U}{\operatorname{argmin}} \|B^{k+1} \otimes U - W\|_2^2 + \lambda_2 \|U - S^k - D_2^k\|_2^2, \quad (7)$$

$$S^{k+1} = \underset{S}{\operatorname{argmin}} \frac{\lambda_2}{2} \|U^{k+1} - S - D_2^k\|_2^2 + \mu_2 \|S\|_0, \quad (8)$$

$$D_2^{k+1} = D_2^k + U^{k+1} - S^{k+1}. \quad (9)$$

In Eq. (3), the auxiliary variables  $Z$  and  $S$  relax the cost function to facilitate minimization with respect to each unknown variable. In Eqs. (4)-(9), the penalty weights  $\lambda_1$  and  $\lambda_2$  are constant and positive, and  $D_1$  and  $D_2$  serve as constraint errors. The split Bregman method permits the penalty weights to remain constant in addition to the benefits of quick convergence and a stable solution.

Problems (4) and (7) are least-square problems whose terms are all quadratic. In accordance with Plancherel's theorem [22], the Fourier transform of the sum of quadratic terms is equal to the sum of the Fourier transforms of each

quadratic term. Thus, in the fast Fourier transform (FFT) domain, Eqs. (4) and (7) can be written respectively as

$$F(B^{k+1}) = \underset{F(B)}{\operatorname{argmin}}\{\|F(B) \odot F(U^k) - F(W)\|_2^2 + \lambda_1\|F(B) - F(Z^k) - F(D_1^k)\|_2^2\}, \quad (10)$$

s.t.  $b_i^{k+1} \geq 0, \Sigma_i b_i^{k+1} = 1$

and

$$F(U^{k+1}) = \underset{F(U)}{\operatorname{argmin}}\{\|F(B^{k+1}) \odot F(U) - F(W)\|_2^2 + \lambda_2\|F(U) - F(S^k) - F(D_2^k)\|_2^2\}, \quad (11)$$

where  $F$  denotes the FFT operation and  $\odot$  represents the scalar product.  $B^{k+1}$  and  $U^{k+1}$ , can be efficiently computed by

$$B^{k+1} = F^{-1}\left(\frac{F^*(U^k) \odot F(W) + \lambda_1 F(E_1)}{F^*(U^k) \odot F(U^k) + \lambda_1}\right) \quad (12)$$

and

$$U^{k+1} = F^{-1}\left(\frac{F^*(B^{k+1}) \odot F(W) + \lambda_2 F(E_2)}{F^*(B^{k+1}) \odot F(B^{k+1}) + \lambda_2}\right), \quad (13)$$

where  $F^{-1}$  is the inverse FFT operation,  $F^*$  is the complex conjugate of  $F$ ,  $E_1 = Z^k + D_1^k$  and  $E_2 = S^k + D_2^k$ , and the division is conducted in an elementwise manner. Eqs. (12) and (13) avoid computationally inefficient matrix multiplications and matrix divisions by using FFTs. Given that  $U$  and  $W$  are gradient images, the number of FFT operations decreases remarkably. Although the  $l_0$ -norm easily leads to an NP-hard problem, problems (5) and (8) can be settled using the closed-form analytical solutions

$$Z^{k+1} = \operatorname{Shrink}(B^{k+1} - D_1^k, \sqrt{\frac{2\mu_1}{\lambda_1}}) \quad (14)$$

and

$$S^{k+1} = \operatorname{Shrink}(U^{k+1} - D_2^k, \sqrt{\frac{2\mu_2}{\lambda_2}}), \quad (15)$$

where  $\operatorname{Shrink}$  is the well-known hard shrinkage operator used to compute  $Z^{k+1}$  and  $S^{k+1}$  in the element-by-element modes, which are defined as

$$\operatorname{Shrink}(a, t) = \begin{cases} = 0 & \text{if } |a| \leq t \\ = a & \text{if } |a| > t. \end{cases} \quad (16)$$

A coarse-to-fine update manner, such as that in [2], is adopted to improve the performance of blur estimation. The blurry images downsampled at different resolutions, together with the blurry image itself, are used to build an image pyramid. At the coarsest level, the pyramid image of lowest resolution is applied to estimate the coarsest-level blur kernel. After the blur kernel obtained at a coarser level is upsampled, it serves as the input for blur estimation at the next-finer level, along with the pyramid image for the corresponding level. At the finest level, the final estimation of the blur kernel is acquired.

Based on the above analysis, the proposed method for blur estimation can be summed up as **Method 1**, shown below.

---

### Method 1 Proposed Method for Blur Estimation

---

**Input:** image pyramid  $\{W_j\}_0^N$  with  $W = W_0$

**Input:** initial  $U_0$  (same size as  $W_N$ )

**Input:**  $\mu_1, \mu_2, \lambda_1$  and  $\lambda_2$

**Output:**  $B^{k+1}$  at finest-level

1: **loop** coarse-to-fine:

2:     **repeat**

3:         Compute  $B^{k+1}$  using Equation (12)

4:         Compute  $U^{k+1}$  using Equation (13)

5:     **until** stopping criterion is met

6:     Upsample  $U^{k+1}$  and  $W$  to initialize next finer level

---

### B. Image Deconvolution

The BID problem becomes an image deconvolution problem, or a non-BID problem, after estimating the blur kernel. Considering the disturbances caused by noise and, possibly, small errors in blur estimation, we model the image deconvolution as the following classic TV-regularized minimization problem to robustly reconstruct the sharp image:

$$\min_X \left\{ \frac{1}{2} \|B \otimes X - Y\|_2^2 + \mu \|\nabla X\|_1 \right\}, \quad (17)$$

where  $\nabla = (\nabla_h, \nabla_v)^T$  is the gradient operator. The TV-regularized model is known to excellently suppress artifacts caused by estimation errors and noise. Various methods can be used to solve Problem (17). The method presented in [23] is employed as the solver because of its processing efficiency and accuracy. This method transforms problem (17) into

$$\min_{X, C} \left\{ \frac{1}{2} \|B \otimes X - Y\|_2^2 + \mu \|C\|_2 + \frac{\beta}{2} \|C - \nabla X\|_2^2 \right\}. \quad (18)$$

Then, problem (18) is solved using a half-quadratic approach with  $\mu$  and  $\beta_0$  equal to  $5 \times 10^4$  and 1, respectively.

## III. EXPERIMENTS AND RESULTS

Experiments are conducted on synthetic and real-world blurry images which are representative and widely adopted to evaluate BID methods. The benchmark images shown in Figs. 1 and 2 are downloaded from open databases [24-26]. The proposed method, along with its three alternatives [4], [10], and [13], are applied to these images, producing deblurred outputs, as illustrated in Figs. 3-9 and Tables I and II. To fairly and objectively conduct the experiments, the results of the three alternatives are obtained by running the source code published by the corresponding authors. Throughout the experiments, the ‘‘stopping criterion’’ in the description of **Method 1** refers to 20 repetitions, and the parameters of the proposed method are set as follows:  $\mu_1 = 0.025$ ,  $\mu_2 = 0.004$ ,  $\lambda_1 = 0.01$ , and  $\lambda_2 = 0.0002$ . When dealing with the images shown in Fig. 2, each method is employed 10 times and, to compare the speeds, the average times are recorded in TABLE I. All the BID methods are executed on a notebook computer equipped with the Windows 7 (64-bit) operating system, MATLAB R2012a (64-bit), Intel Core i5-4258U @ 2.40 GHz, and 4 GB RAM.

**Experiments on Images in Database [24].** The first group of deblurring tests is carried out on a database which contains 32 grayscale images. These images are generated from four sharp benchmark images, shown in Figs. 1(a)-1(d). Each of

the sharp images is blurred with eight different types of kernels, illustrated in Figs. 1(e)-1(l). In the coarse-to-fine procedure, we initialize the sizes of the blur kernels to  $3 \times 3$  and gradually enlarge the sizes to their real values. Eight blurry versions of each sharp image in database [24] are processed by the four BID methods, and the resulting average PSNR values are presented in the histograms in Fig. 3. PSNR is adopted as the objective quantitative criterion of output quality to compare the abilities of the four BID methods. Fig. 3 shows clearly that, when restoring the images in database [24], the proposed method results in the best image quality compared to the other three methods.

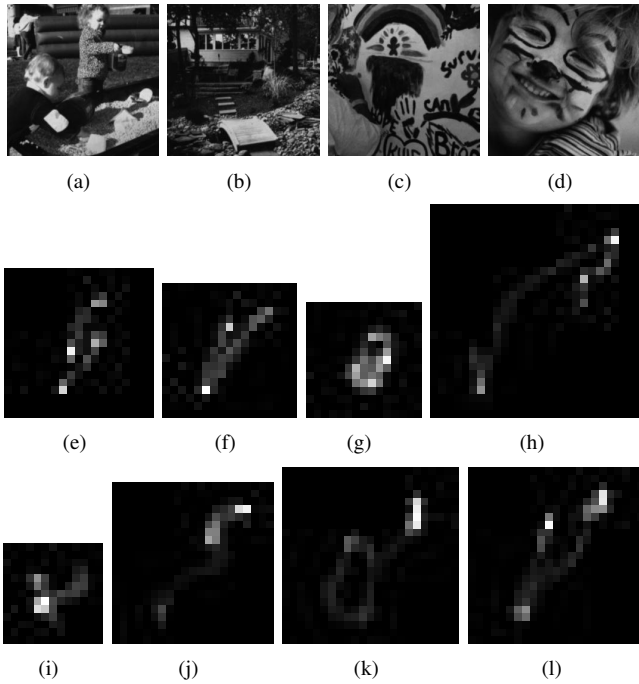


Fig. 1: Sharp Images and Blur Kernels in Database [24]

**Experiments on Images in Database [25].** The second group of deblurring tests are performed on a database containing synthetic blurry color images. In the coarse-to-fine procedure, we update the sizes of the blur kernels in order:  $5 \times 5$ ,  $9 \times 9$ ,  $13 \times 13$ ,  $17 \times 17$ ,  $21 \times 21$ ,  $25 \times 25$  and  $31 \times 31$ . PSNR is also adopted as the objective quantitative criterion of output quality for comparisons, to be utilized after the synthetic blurry images demonstrated in Figs. 2(a) and 2(b) are deblurred. As shown in Tables I and II, the proposed method achieved superior results (i.e., the highest PSNR values) and had the lowest computation time among the four BID methods. This can be visually verified by Fig. 4. When dealing with the synthetic blurry images in Figs. 2(a)-2(b), method [10] only removes part of the blur, and the residual blur negatively influences the visual quality of the deblurred images. Method [13] eliminates the blur in Figs. 2(a)-2(b) well, but it provides oversmooth outputs, erasing some key details. Except for missing a few small details, method [4] recovers more visually pleasing synthetic images than method [13] and benefits from edge enhancement. The proposed method obtained clearer reconstructions of the synthetic blurry images, displaying sharper edges and fewer ring artifacts than its three alternatives.

**Experiments on Images in Database [26].** The third

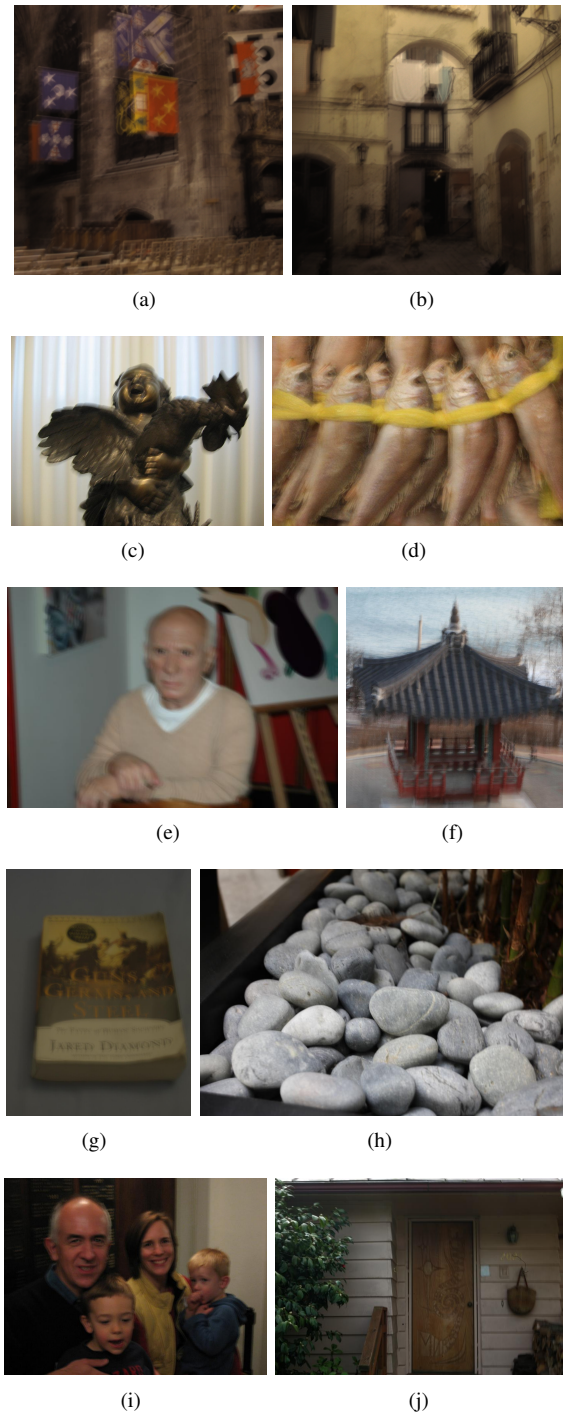


Fig. 2: Blurry Images from Databases [25] and [26]: (a) to (b) Synthetic Blurry Images; (c) to (j) Real-World Blurry Images

group of deblurring tests is carried out on a database containing real-world blurry color images. In the coarse-to-fine procedure, we update the sizes of the blur kernel in the same manner as that in the second group of experiments. As the corresponding ground truth images for the real-world blurry images are unknown, their deblurred results are directly and qualitatively compared and analyzed. As shown in Figs. 5-8, when handling real-world blurry images, conclusive results somewhat differ from the types of results described above. Method [10] fails to remove the most visible blur, which results in notable ring artifacts at the edges of the output.

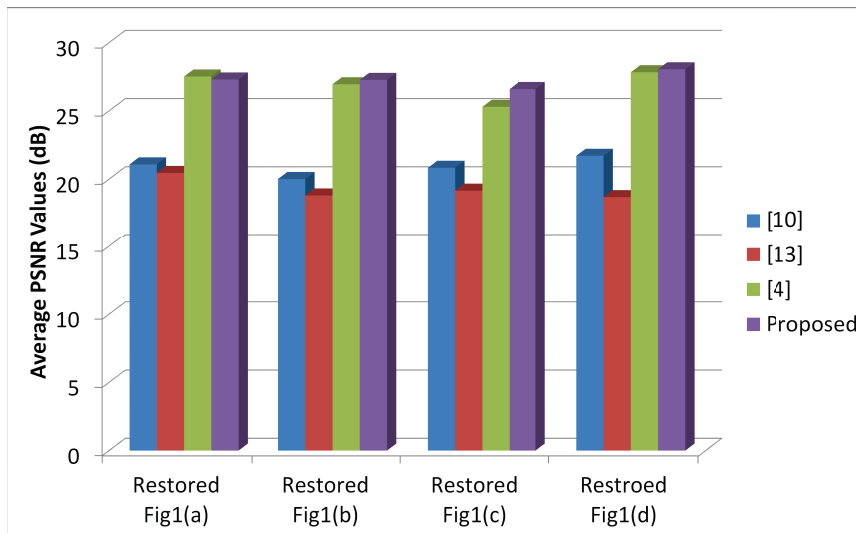


Fig. 3: Average PSNR Values Obtained from Handling the Blurry Images in Database [24]

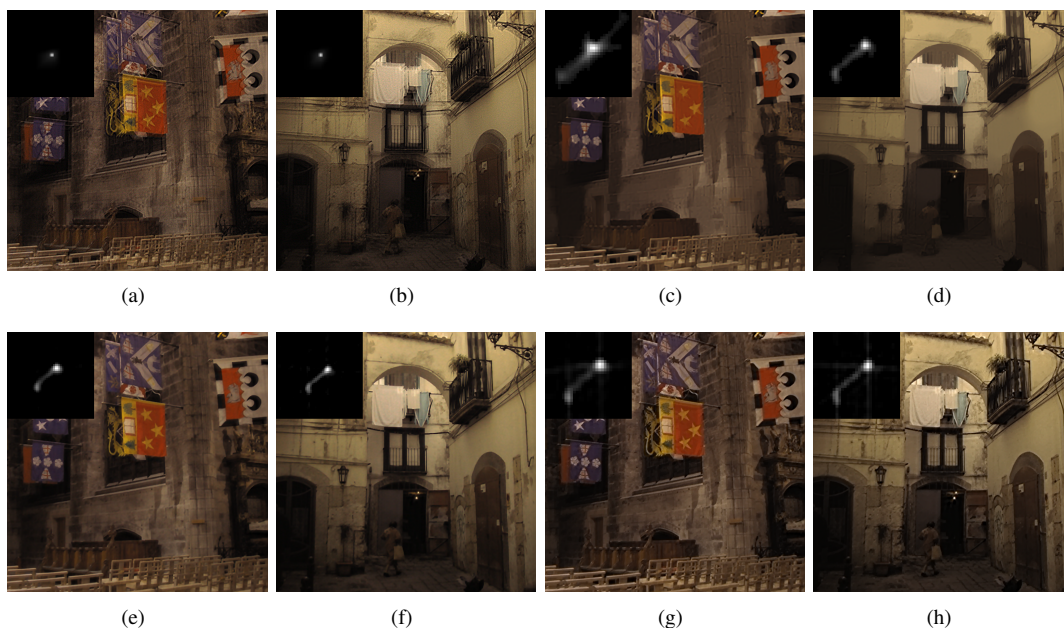


Fig. 4: Restored Sharp Images from Synthetic Blurry Images in Figs. 2(a)-2(b): (a) to (b) Outputs of Method [10]; (c) to (d) Outputs of Method [13]; (e) to (f) Outputs of Method [4]; (g) to (h) Outputs of the Proposed Method

These are shown clearly in Fig. 6(c), Fig. 8(a) and so on. Thus, in the visual sense, its results are inferior to those of the other three methods. Since some of the edges are smoothed out, the real-world sharp images estimated by method [13] seem less natural. Moreover, in Figs. 6(g), Fig. 8(h) and so on, unpleasing blurry edges can be observed. Although method [4] recovers more natural-looking real-world images in contrast to method [13], the residual blur is still visible, as illustrated by Fig. 6(k), Fig. 8(i) and so on. Comparing the images in Figs. 5-8 and the computation times reported in TABLE I, among the four BID methods, the proposed method provides the most visually satisfying output results in the least amount of time. The results have clearer edges, fewer ring artifacts, brighter tones and finer details. To experimentally analyze the convergence of the proposed method, the evolving curves of the cost function when reconstructing sharp images are plotted in Fig. 9. As demonstrated by this figure, the values of cost function

keep decreasing with iteration, indicating that the proposed method converges.

#### IV. CONCLUSION

This study presents an efficient BID method that divides the work of deblurring into two stages. In the first stage, blur estimation was equated to a regularized minimization problem with constraints. The split Bregman method, FFTs, and a hard shrinkage approach were combined to resolve the blur estimation problem in a coarse-to-fine updating procedure. In the second stage, since the blur kernel was known, the reconstruction of the sharp image was treated as an image deconvolution problem and represented by the classic TV-regularized model. An efficient classic method based on half-quadratic regularization was employed to resolve the image deconvolution problem. In the experimental section, a set of synthetic blurry images and real-world blurry images were

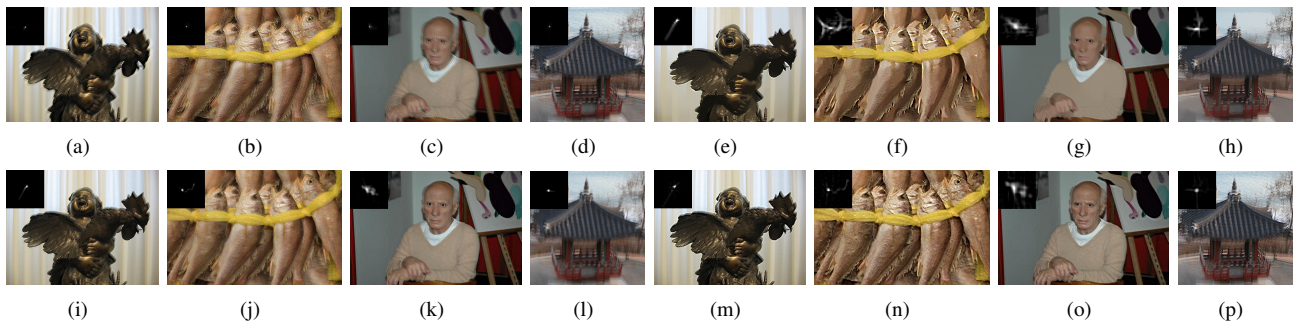


Fig. 5: Processing Results for the Blurry Images in Figs. 2(c)-2(f): (a) to (d) Outputs of Method [10]; (e) to (h) Outputs of Method [13]; (i) to (l) Outputs of Method [4]; (m) to (p) Outputs of the Proposed Method

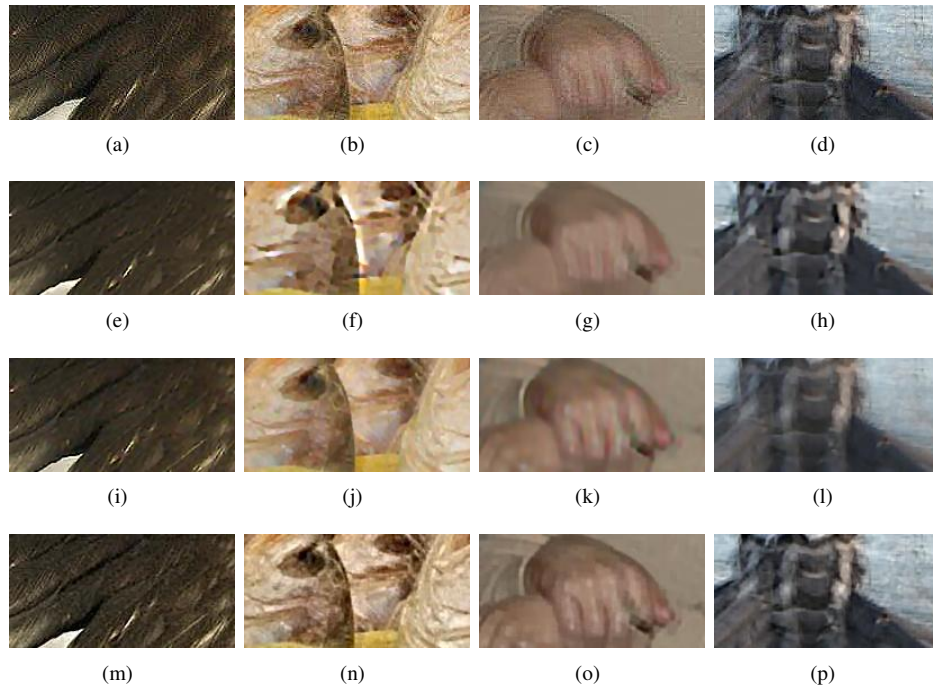


Fig. 6: Local Regions of the Reconstructed Sharp Images in Fig. 5: (a) to (d) Local Regions of the Outputs of Method [10]; (e) to (h) Local Regions of the Outputs of Method [13]; (i) to (l) Local Regions of the Outputs of Method [4]; (m) to (p) Local Regions of the Outputs of the Proposed Method

TABLE I: Average Time (seconds) for Dealing with the Blurry Images in Fig. 2

Methods	Fig. 2(a)	Fig. 2(b)	Fig. 2(c)	Fig. 2(d)	Fig. 2(e)	Fig. 2(f)	Fig. 2(g)	Fig. 2(h)	Fig. 2(i)	Fig. 2(j)
[10]	6291.44	6219.64	8314.26	4776.20	4005.39	9496.43	7673.92	6013.82	3118.42	2578.63
[13]	654.55	674.43	765.56	613.69	399.02	621.33	651.60	285.17	217.67	156.83
[4]	305.69	314.85	980.08	475.63	159.85	1140.50	305.88	382.05	121.37	300.41
Proposed	284.26	263.87	277.90	216.50	141.22	395.52	139.87	206.37	115.49	109.89

deblurred by the proposed method and three similar state-of-the-art methods. The experimental results demonstrated that the proposed method accomplished deblurring tasks more quickly and accurately than the three alternatives.

#### REFERENCES

- [1] A. C. Likas and N. P. Galatsanos, "Variational approach for Bayesian blind image deconvolution," *IEEE Transactions on Signal Processing*, vol. 52, no. 8, pp. 2222-2233, Aug. 2004.
- [2] R. Fergus, B. Singh, A. Hertzmann, S. T. Roweis and W. T. Freeman, "Removing camera shake from a single photograph," *ACM Transactions on Graphics*, vol. 25, no. 3, pp. 787-794, Jul. 2006.
- [3] D. G. Tzikas, A. C. Likas and N. P. Galatsanos, "Variational Bayesian sparse kernel-based blind image deconvolution with students-t priors," *IEEE Transactions on Image Processing*, vol. 18, no. 4, Apr. 2009.
- [4] X. Zhou, J. Mateos, F. Zhou, R. Molina and A. K. Katsaggelos, "Variational Dirichlet blur kernel estimation," *IEEE Transactions on Image Processing*, vol. 24, no. 12, pp. 5127 - 5139, Dec. 2015.
- [5] T. F. Chan and C. Wong, "Total variation blind deconvolution," *IEEE Transactions on Image Processing*, vol. 7, no. 3, pp. 370-375, Mar. 1998.
- [6] W. Li, Q. Li, W. Gong and S. Tang, "Total variation blind deconvolution employing split Bregman iteration," *Journal of Visual Communication and Image Representation*, vol. 23, no. 3, pp. 409-417, Apr. 2012.
- [7] G. Liu, S. Chang and Y. Ma, "Blind image deblurring using spectral properties of convolution operators," *IEEE Transactions on Image Processing*, vol. 23, no. 12, pp. 5047-5056, Dec. 2014.
- [8] H. Liu, J. Gu, M. Q. H. Meng and W. S. Lu, "Fast weighted total variation regularization algorithm for blur identification and image restoration," *IEEE Access*, vol. 4, pp. 6792-6801, Jan. 2016.

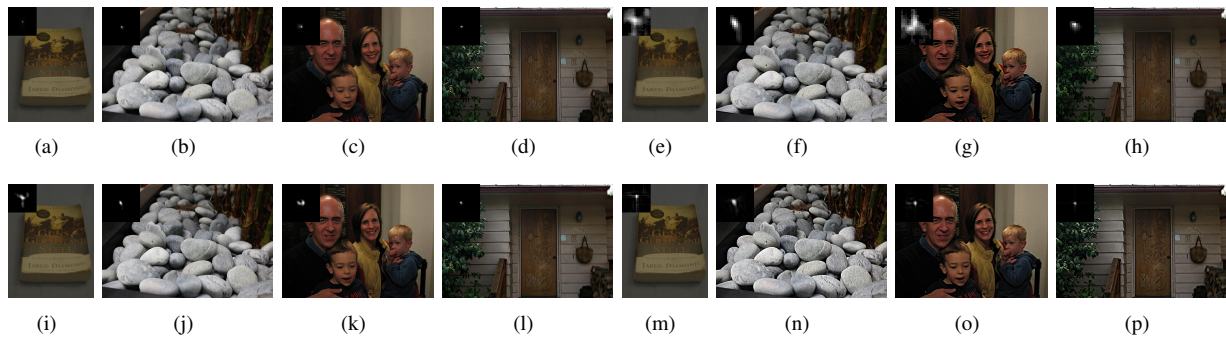


Fig. 7: Processing Results for the Blurry Images in Figs. 2(g)-2(j): (a) to (d) Outputs of Method [10]; (e) to (h) Outputs of Method [13]; (i) to (l) Outputs of Method [4]; (m) to (p) Outputs of the Proposed Method

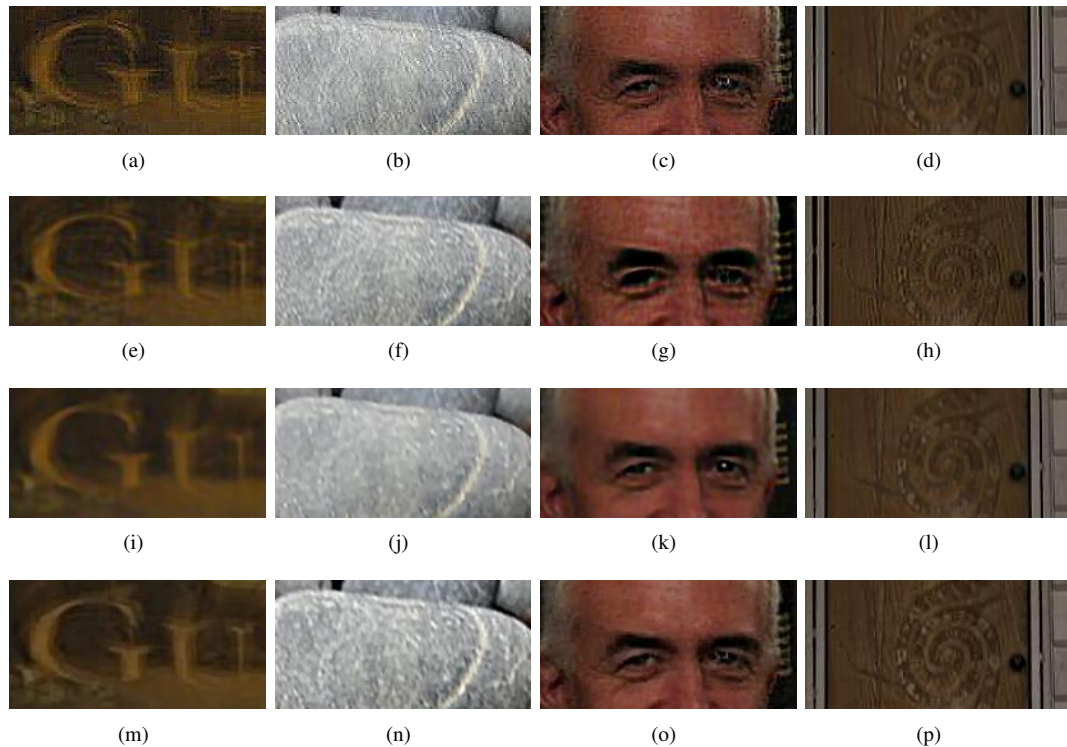


Fig. 8: Local Regions of the Reconstructed Sharp Images in Fig. 7: (a) to (d) Local Regions of the Outputs of Method [10]; (e) to (h) Local Regions of the Outputs of Method [13]; (i) to (l) Local Regions of the Outputs of Method [4]; (m) to (p) Local Regions of the Outputs of the Proposed Method

TABLE II: PSNRs (dB) of the Estimated Sharp Synthetic Images in Fig. 4

Images	Fig. 4(a)	Fig. 4(b)	Fig. 4(c)	Fig. 4(d)	Fig. 4(e)	Fig. 4(f)	Fig. 4(g)	Fig. 4(h)
PSNRs	24.30	24.51	28.33	32.57	30.39	33.56	32.42	33.85

- [9] D. Perrone and P. Favaro, "A clearer picture of total variation blind deconvolution," *IEEE Transactions on Pattern Analysis and Machine Intelligence*, vol. 38, no. 6, pp. 1041-1055, Jun. 2016.
- [10] J. F. Cai, H. Ji, C. Liu and Z. Shen, "Framelet-based blind motion deblurring from a single image," *IEEE Transactions on Image Processing*, vol. 21, no. 2, pp. 562-572, Feb. 2012.
- [11] W. Ren, J. Tian and Y. Tang, "Blind deconvolution with nonlocal similarity and  $l^0$  sparsity for noisy image," *IEEE Signal Processing Letters*, vol. 23, no. 4, pp. 439-443, Apr. 2016.
- [12] J. Yu, Z. Chang, C. Xiao and W. Sun, "Blind image deblurring based on sparse representation and structural self-similarity," in *Proceedings of IEEE International Conference on Acoustics, Speech and Signal Processing*, New Orleans, LA, USA, 2017, pp. 1328-1332.
- [13] J. Pan, Z. Hu, Z. Su and M. H. Yang, "Deblurring text images via  $L_0$ -regularized intensity and gradient prior," in *Proceedings of IEEE Conference on Computer Vision and Pattern Recognition*, Columbus, OH, USA, 2014, pp. 2901-2908.
- [14] A. N. Tikhonov, A. Goncharky, V. V. Stepanov and A. G. Yagola, *Numerical Methods for the Solution of Ill-Posed Problems*. New York: Springer, 1995.
- [15] S. Cho and S. Lee, "Fast motion deblurring," *ACM Transactions on Graphics*, vol. 28, no. 5, Dec. 2009.
- [16] T. Goldstein and S. Osher, "The split Bregman method for L1-regularized problems," *SIAM Journal on Imaging Sciences*, vol. 2, no. 2, pp. 323-343, Apr. 2009.
- [17] G. Hou, G. Wang, Z. Pan, B. Huang, H. Yang and T. Yu, "Image enhancement and restoration: state of the art of variational retinex models," *IAENG International Journal of Computer Science*, vol. 44, no. 4, pp. 445-455, Nov. 2017.
- [18] S. Osher, M. Burger, D. Goldfarb, J. Xu and W. Yin, "An iterative regularization method for total variation-based image restoration," *Multiscale Modeling and Simulation*, vol. 4, no. 2, pp. 460-489, Jul. 2006.
- [19] J. Yan and W. S. Lu, "Image denoising by generalized total variation

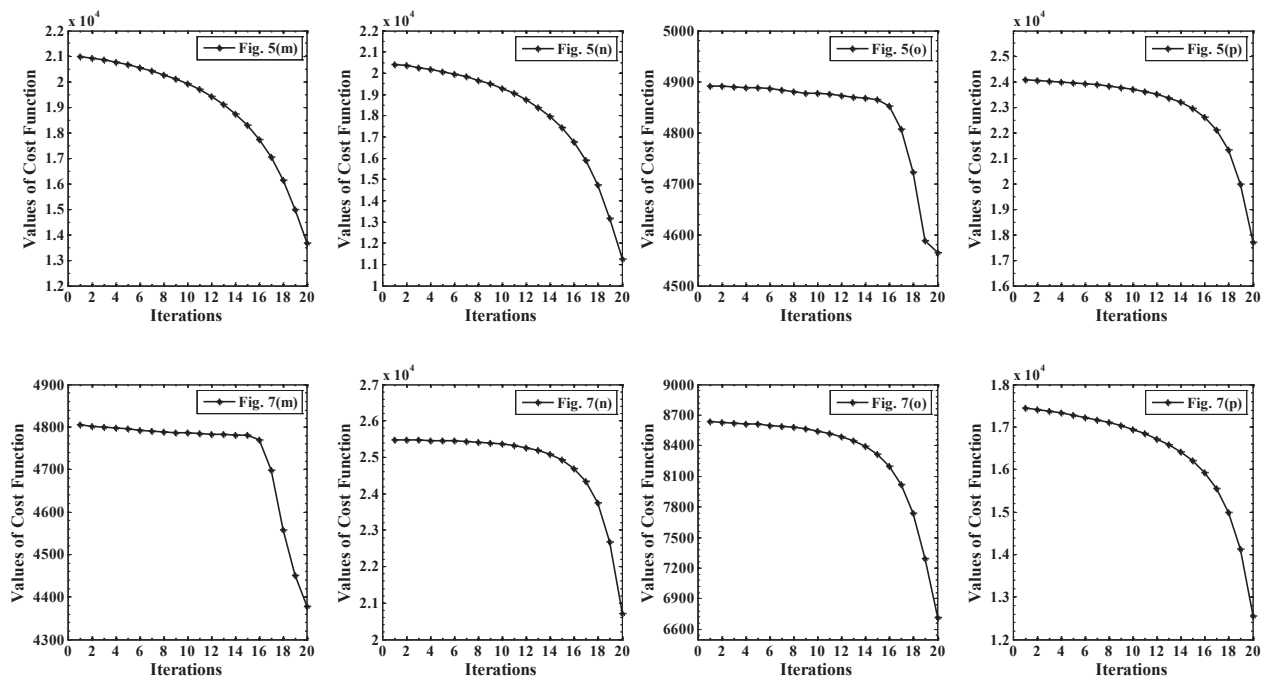


Fig. 9: Value Variations of the Cost Function When Producing Sharp Images

- regularization and least squares fidelity,” *Multidimensional Systems and Signal Processing*, vol. 26, no. 1, pp. 243-266, Jan. 2015.
- [20] J. Duan, Z. Pan, B. Zhang, W. Liu and X. C. Tai, “Fast algorithm for color texture inpainting using the non-local CTV model,” *Journal of Global Optimization*, vol. 62, no. 4, pp. 853-876, Aug. 2015.
- [21] P. Yin, Y. Lou, Q. He and J. Xin, “An iterative regularization method for total variation-based image restoration,” *SIAM Journal on Scientific Computing*, vol. 37, no. 1, pp. A536-A563, Feb. 2015.
- [22] R. N. Bracewell, *The Fourier Transform & Its Applications*. New York: McGraw-Hill, 1999.
- [23] Y. Wang, J. Yang, W. Yin and Y. Zhang, “A new alternating minimization algorithm for total variation image reconstruction,” *SIAM Journal on Imaging Sciences*, vol. 1, no. 3, pp. 248-272, Aug. 2008.
- [24] A. Levin, Y. Weiss, F. Durand and W. T. Freeman, “Understanding and evaluating blind deconvolution algorithms,” *Proceedings of IEEE Conference on Computer Vision and Pattern Recognition*, Miami, FL, USA, 2009, pp. 1964-1971.
- [25] R. Kohler, M. Hirsch, B. Mohler, B. Scholkopf and S. Harmeling, “Recording and playback of camera shake: benchmarking blind deconvolution with a real-world database,” in *Proceedings of European Conference on Computer Vision*, Florence, Italy, 2012, pp. 27-40.
- [26] W. S. Lai, J. B. Huang, Z. Hu, N. Ahuja and M. H. Yang, “A comparative study for single image blind deblurring,” in *Proceedings of IEEE Conference on Computer Vision and Pattern Recognition*, Las Vegas, NV, USA, 2016, pp. 1701-1709.